

# Porosity Dependence of Compression and Lattice Rigidity in Metal-Organic Framework Series

Louis R. Redfern<sup>†‡</sup>, Lee Robison<sup>†</sup>, Megan C. Wasson<sup>†</sup>, Subhadip Goswami<sup>†</sup>, Jiafei Lyu<sup>†</sup>, Timur Islamoglu<sup>†</sup>, Karena W. Chapman<sup>‡§\*</sup>, and Omar K. Farha<sup>†\*</sup>

<sup>†</sup> Department of Chemistry, Northwestern University, 2145 Sheridan Rd., Evanston, IL 60208-3113

<sup>‡</sup> X-ray Science Division, Advanced Photon Source, Argonne National Laboratory, Lemont, Illinois 60439-4858, United States

<sup>§</sup> Department of Chemistry, Stony Brook University, 100 Nicolls Rd., Stony Brook, NY 11794

\*Corresponding Authors. Email: o-farha@northwestern.edu, karena.chapman@stonybrook.edu

---

**ABSTRACT:** Porous materials, including metal-organic frameworks (MOFs), are known to undergo structural changes when subjected to applied hydrostatic pressures that are both fundamentally interesting and practically relevant. With the rich structural diversity of MOFs, the development of design rules to better understand and enhance the mechanical stability of MOFs is of paramount importance. In this work, the compressibilities of seven MOFs belonging to two topological families (representing the most comprehensive study of this type to date) were evaluated using *in situ* synchrotron X-ray powder diffraction of samples within a diamond anvil cell. Judicious selection of these materials, representing widely-studied classes of MOFs, provides broadly applicable insight into the rigidity and compression of hybrid materials. Analysis of these data reveals that the bulk modulus depends on several structural parameters (*e.g.* void fraction and linker length). Furthermore, we find that lattice distortions play a major role in the compression of MOFs. This study is an important step toward developing a predictive model of the structural variables that dictate the compressibility of porous materials.

---

## INTRODUCTION

Over the past two decades, advances in the design and synthesis of metal-organic frameworks (MOFs) have enabled diverse applications, including, but not limited to, gas adsorption, chemical separations, and heterogeneous catalysis.<sup>1-5</sup> Their open structures are formed by inorganic nodes connected by multitopic organic linkers to form diverse two- and three-dimensional frameworks.<sup>6</sup> The guest-accessible voids defined by the MOF lattice can impart counterintuitive structural phenomena, such as framework flexibility under mild stimuli,<sup>7-8</sup> guest-dependent compression behavior,<sup>9</sup> and unit cell expansion upon application of external pressure.<sup>10</sup> While pressure-induced structural changes are fascinating, systematic studies to identify design rules for such phenomena are complicated by the rich structural diversity of MOFs and the multitude of variables that dictate their chemical and physical properties (*e.g.* topology, connectivity, ligand length, void fraction, disorder, defect density, *etc.*). Due to the interdependence of these structural parameters, it is challenging to define a well-controlled series of MOFs in which a single variable is modified while all others are held constant, yet this type of rigorous experimental design is essential to draw conclusions that can be extended to predict the properties of other materials. Despite these challenges, understanding the compression of MOFs is fundamentally important and crucial for the development of design rules to enhance

their mechanical stability for practical applications requiring high pressures, such as the formation of pellets or extrudates.

The intimate relationship between structure and function in porous materials—such as zeolites, zeolitic imidazolate frameworks (ZIFs), and MOFs—has motivated much research into the behavior of these materials under pressure. The earliest high-pressure studies of zeolites revealed that molecules from the hydrostatic fluid that acts as the pressure transmitting medium can infiltrate the pore network to moderate the observed compression of porous systems.<sup>11</sup> Additional studies indicate that increased porosity does not directly correlate to an increase in the compressibility of the material, and that some microporous zeolites have higher bulk moduli than non-porous, rock-forming minerals.<sup>12-13</sup> Despite many similarities, the insights into zeolite behaviors under pressure may not be straightforwardly extended to MOFs owing to the distinct chemical nature of the two classes of materials. Early studies of compression in ZIFs reveal rapid amorphization and modified porosity upon pressure treatment.<sup>14</sup> Nanoindentation studies of ZIFs reveal that the elastic modulus is related to the density of the framework.<sup>15</sup> Further, it has been shown computationally<sup>16</sup> and experimentally<sup>17</sup> that higher density ZIFs are more thermodynamically stable. Recently, the pressure response of several MOFs has been investigated with primarily computational approaches, supporting general trends found in ZIFs and zeolites,<sup>18-19</sup> though

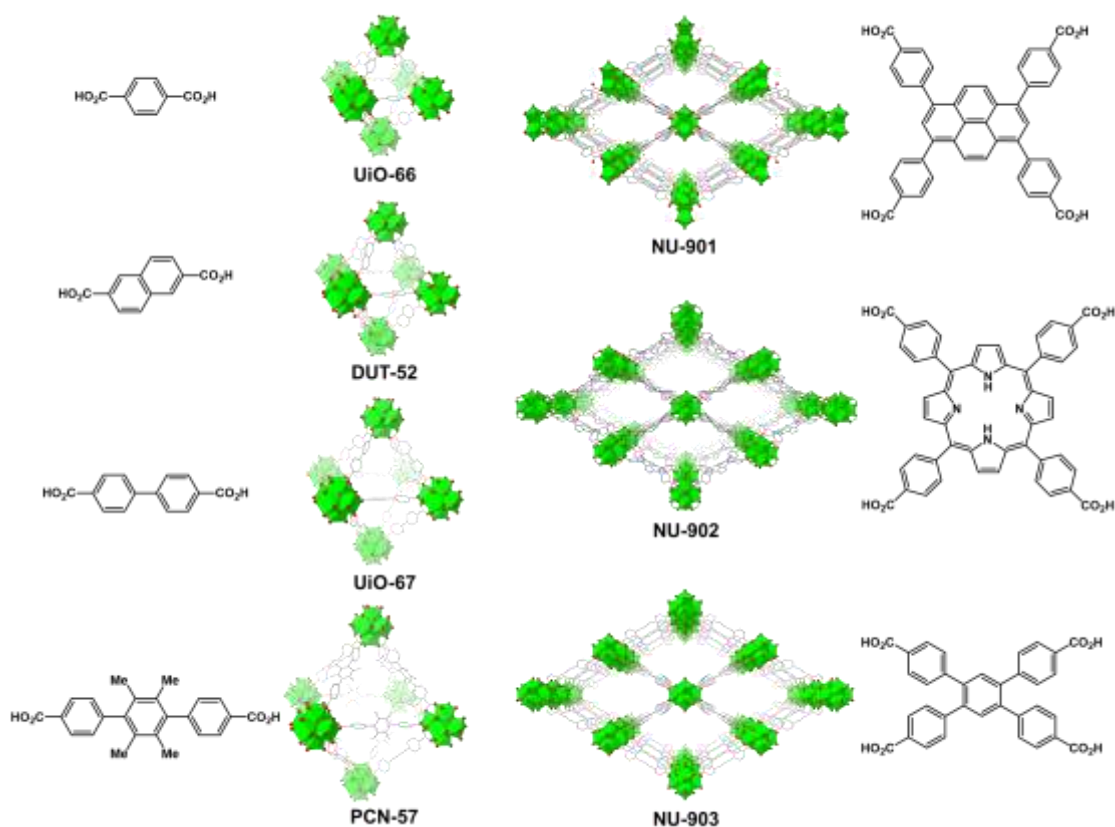


**Figure 1.** MOF structures and linkers of the isorecticular UiO and NU-900 series used in this study.

this diverse class of materials offers many underexplored structure-property relationships. While existing reports on the pressure-dependent behavior of MOFs have mainly focused on extensively investigating individual examples, more broad studies of different MOF families are notably lacking. The similarities and differences among zeolites, ZIFs, and MOFs demonstrate the importance of such studies for understanding the compression of all classes of porous materials.

In this work, we investigate the impact of modest pressures (<0.5 GPa, which can be encountered routinely in practical applications) on the structure of seven Zr-based MOFs in two topological families (**Figure 1**): the UiO series (UiO-66, DUT-52, UiO-67, PCN-57 [a structural analogue of UiO-68]) and the NU-900 series (NU-901, NU-902, and NU-903). These carefully selected materials allow us to probe the effects of modulating the organic linker within the *fcu* and *scu* topologies, while simultaneously comparing how different topologies influence the pressure response of these MOFs. To our knowledge, this is the most extensive experimental study of compression in MOFs to date (seven examples across two families), and it is the first work to investigate the high-pressure behavior of *scu*-topology MOFs, as well as DUT-52 and PCN-57. Our results reveal that some trends, such as the nearly-quantitative relationship between void fraction and compressibility, are conserved across both families, while other variables (such

as linker length) exhibit qualitatively different impacts on the two topologies. Additionally, we discuss the behavior of two examples in the UiO family which help to identify secondary structural characteristics that influence compressibility. In total, these observations provide guiding principles to predict the pressure response of MOFs and other porous materials, while gaining valuable insight into the compression mechanism of these materials.

#### EXPERIMENTAL SECTION

The seven MOFs discussed herein are comprised of di- or tetracarboxylate ligands and identical Zr<sub>6</sub> nodes, resulting in a collection of materials that differ only in topology and linker geometry. Isolating the role of the organic linker in this way ensures that observed structure-property relationships are generalizable to a variety of other MOFs. The well-studied UiO MOFs are comprised of 12-connected Zr<sub>6</sub>O<sub>8</sub> clusters joined by linear ditopic organic ligands of various lengths to form a framework of tetrahedral and octahedral cages in the *fcu* topology. The NU-900 series is constructed from 8-connected Zr<sub>6</sub>O<sub>8</sub> nodes with planar tetratopic linkers with differing sizes and aspect ratios arranged in the *scu* topology, giving rise to diamond shaped channels connected by small windows. Each series of MOFs was synthesized and activated according to modified literature procedures (see SI for details).<sup>20-25</sup> Because defect density in porous materials has been shown to impact their physical properties (such as thermal stability in

**Table 1: Summary of bulk moduli and key structural parameters for the studied MOFs.**

MOF	Bulk Modulus (GPa)	Void fraction <sup>a</sup>	Nearest Node Distance (Å)	Linker Length (Å) <sup>b</sup>	Ambient Pressure Node-Node Contraction (Å) <sup>c</sup>
UiO-66	37.9(6)	0.53	14.83	6.02	0.001
DUT-52	17(2)	0.57	16.91	7.99	0.05
UiO-67	21.1(6)	0.64	19.16	10.09	0.006
PCN-57	4.6(1)	0.73	23.57	14.35	0.09
NU-901	7.2(3)	0.70	16.05	17.08	--
NU-902	6.8(1)	0.73	17.12	18.56	--
NU-903	12.2(4)	0.66	11.19	14.34	--

<sup>a</sup>Void fraction values estimated in PLATON. <sup>b</sup>Linker lengths are measured as the C-C distance for carboxylates located farthest apart on a single linker in reported crystal structures. <sup>c</sup>See SI for details regarding determination of node-node contraction.

zeolites<sup>26</sup> and compression of MOFs<sup>27</sup>), particular efforts were taken to minimize defects in these samples. The materials were characterized *via* powder X-ray diffraction and nitrogen isotherm experiments to verify their crystallinity, porosity, and low defect density in line with previously published reports<sup>21-23, 25, 28-30</sup> (See SI, Figures S1-S5).

The compression behavior of each MOF was probed using synchrotron-based powder X-ray diffraction in a diamond anvil cell sample environment. *In situ* X-ray diffraction data ( $\lambda = 0.45240 \text{ \AA}$ ) were collected at the 17-BM beamline of the Advanced Photon Source, Argonne National Laboratory. Le Bail analysis was performed to determine the unit cell parameters of the sample at each pressure. Studying high-pressure behavior in porous materials requires special considerations when selecting a suitable pressure transmitting medium. Typical mixtures of small-molecule fluids, like methanol/ethanol/water, can complicate interpretation of the observed behavior with pressure-induced adsorption, causing the framework to initially swell (or resist compression) and exhibit significantly different pressure response than samples in which a non-penetrating fluid is used.<sup>31-32</sup> For this reason, we select Fluorinert™ FC-70 as an appropriate large-molecule, non-penetrating pressure transmitting fluid for all experiments (see SI for experimental details).

## RESULTS

While Zr-based MOFs are well known for their robust thermal and chemical stability,<sup>33</sup> their structural rigidity under pressure varies significantly. Though pressure-induced peak broadening precludes the application of Rietveld refinements, Le Bail refinement of powder diffraction data collected at various pressures (0-0.5 GPa) reveals the drastically different compressibilities (spanning nearly an order of magnitude) of UiO-66, DUT-52, UiO-67, and PCN-57. The observed decrease in the lattice volume can be modeled using a second-order Birch-Murnaghan equation of state (Figure 2a) to estimate the bulk modulus of each material, which is inversely proportional to the material's compressibility. The same analysis was applied to the NU-900 family (Figure 2b), allowing for comparison within and between the two series. The range of usable data is limited due to the low pressure-range over which

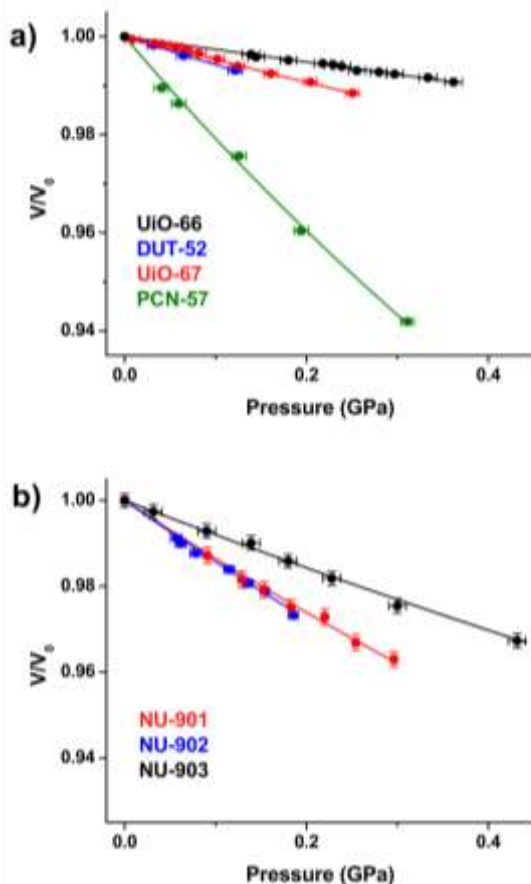


**Figure 2.** Relative lattice compression of (a) the UiO series and (b) the NU-900 series. Lines represent the second-order Birch-Murnaghan equation-of-state fits to the data.

the pressure-transmitting medium remains hydrostatic (i.e. completely fluid) and the amorphization of the MOFs under the additional deviatoric strain beyond the hydrostatic limit of the fluid medium. Notably, the lattice volumes of DUT-52 do not fit well to this model beyond 0.15 GPa. This deviation may indicate a structural transition that follows a different equation of state, inviting further study; however, for the scope of this investigation, we focus on the initial behaviors of the MOFs.

The bulk modulus and several pertinent structural properties of each MOF under ambient conditions are listed in **Table 1**. The bulk moduli of the MOFs studied cover a large range (from 4.6 – 37.9 GPa), comparable to that of sodium metal (6.2 GPa)<sup>34</sup> and quartz (38 GPa),<sup>35</sup> exemplifying the significance of minor structural changes on the pressure response of each material.

## DISCUSSION

Initial comparison of the bulk moduli reveals that as the void fraction increases, the bulk modulus decreases (**Figure 3a**). The consistency of this void fraction dependence in both series indicates that porosity plays an important role in compression of MOFs regardless of topology. This observation supports a model of compression in which the steric repulsion of the framework components is a primary source of lattice rigidity, as increased void space can accommodate greater distortions without causing collisions between linkers or nodes. While void fraction is a good predictor for the bulk moduli of six of the materials studied, DUT-52 exhibits a notably lower bulk modulus than expected based on the void fraction of the other MOFs.

As with void fraction, the bulk modulus generally decreases as nearest node distance and linker length increase; however, the dependence upon these variables is different in each topology (**Figures 3b and 3c**). This difference likely stems from the different dimensionality of the ligand in each family (linear ditopic vs. planar tetratopic), as the nearest nodes are not directly opposed on the linker. Interestingly, while the linker for NU-903 and PCN-57 have nearly identical lengths, the bulk modulus of NU-903 is 7.6 GPa greater. This observation can be rationalized by considering the support of the additional carboxylate groups present in the NU-903 linker. Based on these results, we anticipate that the rigidity of MOFs with large linkers will be enhanced by additional node-binding groups, while decreasing the nearest node distance enhances rigidity for structures with shorter, linear linkers.

Based solely on the compressibility and linker length of the other members of the UiO family, DUT-52 is expected to have a bulk modulus of approximately 30 GPa, but it was experimentally determined to be 17(2) GPa—a value lower than that of UiO-67, despite having a shorter linker length and lower void fraction. This exceptionally low value is likely due an offset in the orientation of the carboxylate groups in the organic ligand causing the linker to be rotated slightly to maintain proper orientation of the inorganic nodes within the MOF—that is, the ligand is not centered on a straight line between nodes. Inspection of the atomic structure model of DUT-52 reveals disorder of the linker between two possible orientations,<sup>21</sup> each rotated approximately 10° from the linear path between the Zr nodes (see SI, **Figure S9**). Unlike UiO-66 and UiO-67, whose linkers maintain linear connectivity despite twisting of the phenyl groups, the deviation from linearity in DUT-52 provides a preferential pathway for compression of the framework, significantly impacting the bulk modulus.

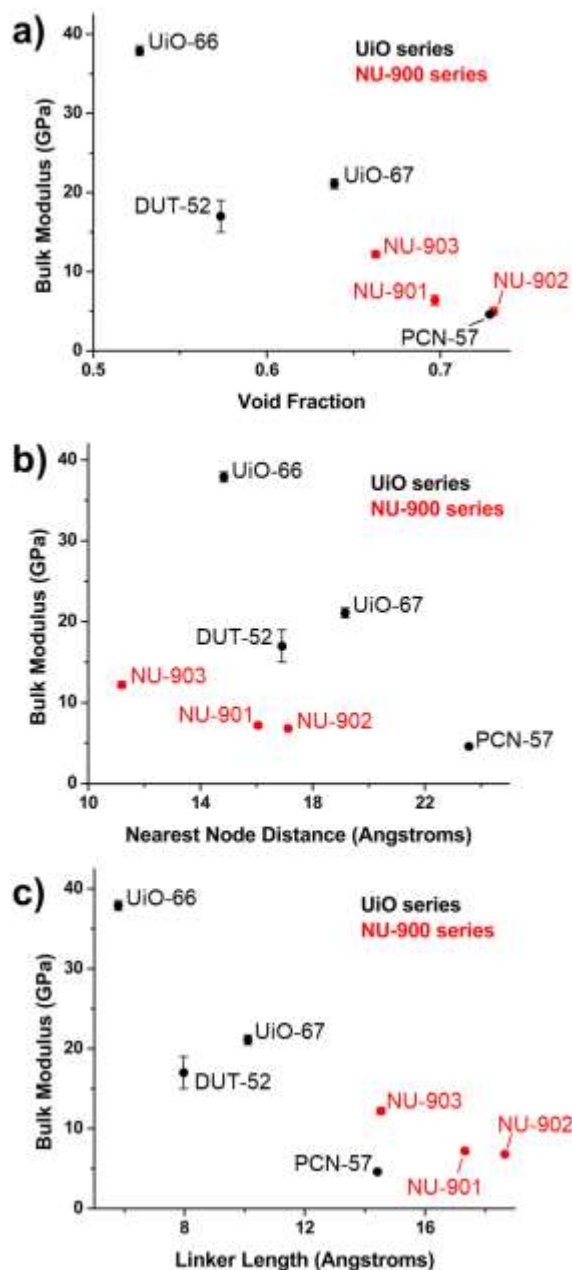


**Figure 3.** Relationship between the bulk modulus and (a) void fraction, (b) nearest node distance, and (c) linker length of the UiO (black) and NU-900 (red) families.

PCN-57 exhibits the lowest bulk modulus of the materials examined in this study (4.6(1) GPa). While we hypothesized that PCN-57 would be more readily compressed than the other members of the UiO family, the observed bulk modulus is significantly lower than that which has been previously estimated from computational simulations of a structurally analogous MOF, UiO-68 (14.4 GPa).<sup>36</sup> Contrarily, experimental values for the bulk modulus of UiO-66 and UiO-67 are in good agreement with computational values from the same study. (38 vs. 41 GPa for UiO-66, and 21 vs. 25 GPa for UiO-67). The discrepancy between PCN-57 and UiO-68 bulk moduli can again be rationalized by considering the reported atomic structure models of

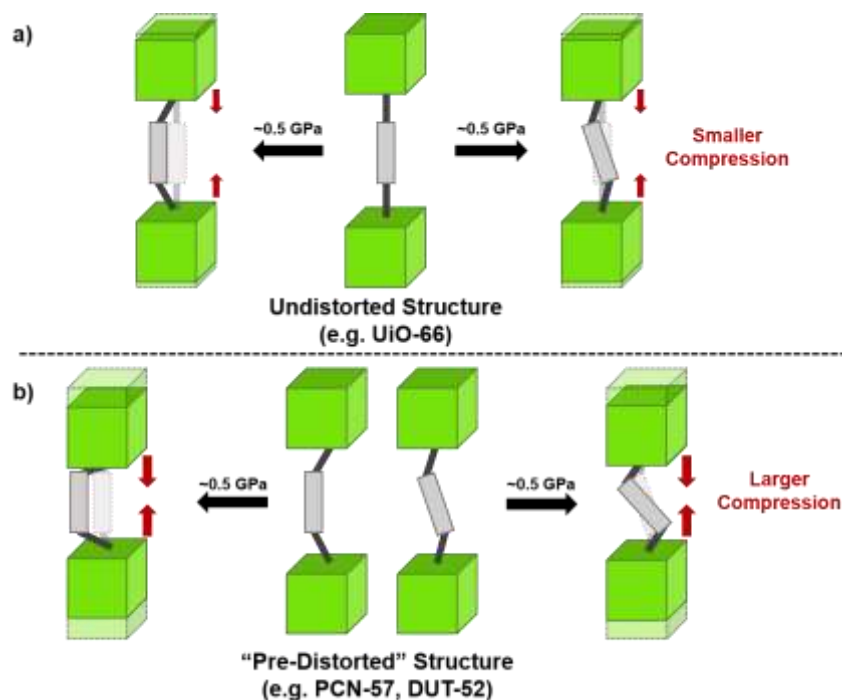


**Figure 4.** (a) MOFs with undistorted structures are more resistant to compression than (b) those with “pre-distorted” structures.

each material. A computational model of UiO-68 has a lattice parameter of  $33.3310 \text{ \AA}$ ,<sup>37</sup> and with identical linker length and node size, PCN-57 should have a nearly identical unit cell; however, at ambient pressure, the lattice parameter of PCN-57 was found to be  $32.872(3) \text{ \AA}$ . The shortening of the lattice parameter by  $0.438 \text{ \AA}$  is due to the ditopic linker bending out of plane (see SI, **Figure S10**), as is evidenced by the increasingly large atomic displacement parameters for carbons toward the center of the linker in the crystal structure of PCN-57 (See SI, **Table S8**).<sup>22</sup> This flexing of the ligand at ambient pressure provides a preferred pathway for compression, leading to a lower bulk modulus than is predicted for the more linear UiO-68 model system.

It has previously been shown that MOFs are most robust in their undistorted geometry and that the bending of the organic linkers away from linear connectivity weakens the framework, resulting in a negative pressure dependence of the bulk modulus ( $K'$ ).<sup>14</sup> In materials with significant linker bending or twisting, such as PCN-57 and DUT-52, a portion of the linkers populate these distortion modes in the absence of external pressure. This produces a subtle node-node contraction (**Table 1**), effectively generating a “pre-distorted” structure that resembles a compressed linear framework. This ambient pressure distortion compromises the strength of the framework, resulting in higher compressibility than would be expected based on other structural parameters, such as void fraction or linker length (**Figure 4**). Based on our analysis of PCN-57 and DUT-52, it is evident that slight differences in MOF structures have profound effects on the pressure response of the material. We hypothesize that the impact of “pre-distortion” of the structure on the bulk modulus can be applied

to other MOFs to provide a useful metric for anticipating which materials will deviate from more general structural trends.

The relationships discussed above provide important insight into the mechanism of compression in MOFs. A number of factors may contribute to the pressure-response, including (i) compression of the node, (ii) flexibility of the node-ligand coordination, (iii) bond length contraction in the linker, and (iv) flexibility of the linker. Due to the identical  $\text{Zr}_6$  node present in these materials and the high bulk modulus of  $\text{ZrO}_2$ , compression of the node is not expected to contribute significantly to the observed trends in lattice compression. Likewise, the carboxylate binding groups shared across each material maintains a consistent flexibility of node-ligand coordination. Although longer linkers exhibit slightly greater compression than shorter linkers at the same node-linker bond angle, this difference is minimal at bond angles expected to be achieved in this study. Bond length contraction may play a role in compression, though we do not expect it to be a significant factor because bond stretching modes are much higher in energy than bond bending modes. In fact, for C-C bond length contraction to account for the observed change in lattice parameter at  $0.3 \text{ GPa}$ , each bond in PCN-57 would need to compress more than four times the amount of those in UiO-66. We therefore propose that compression in these MOFs occurs primarily through linker distortion and is dependent on the linker flexibility. Compression in this way requires void space to accommodate linker deformations, which explains the strong correlation between bulk modulus and void fraction, along with previous findings that solvated MOFs exhibit drastically higher bulk moduli than

their solvent-free (high void volume) counterparts.<sup>9</sup> Furthermore, compression *via* linker distortion provides a rational explanation for the pressure-response of all seven examples investigated in this work. This finding that linker distortion is a major component of compression in MOFs is crucial to understand and predict the behavior of other porous materials under pressure.

## CONCLUSIONS

This study investigates the structural changes of two series of isoreticular MOFs in response to moderate pressures (< 0.5 GPa), which are routinely achieved during post-synthetic processing such as pelletization or extrusion of MOF materials.<sup>38</sup> Powder X-ray diffraction data were collected as a function of pressure within a diamond anvil cell using synchrotron radiation at the Advanced Photon Source at Argonne National Laboratory. Lattice parameters were determined *via* Le Bail analysis, and unit cell compression was modeled using a second-order Birch-Murnaghan equation of state to estimate the bulk modulus of each MOF. The materials studied exhibit a large range of bulk moduli (4–38 GPa). In both topologies studied, the bulk modulus decreases as void fraction, nearest node distance, and linker length increase; however, the dependence of the bulk modulus on nearest node distance and linker length varies between the two families, likely due to differences in linker dimensionality and topology. Interestingly, distortions in the linkers of DUT-52 and PCN-57 at ambient pressure provide a preferential pathway for compression, significantly decreasing the observed bulk modulus of these materials. These results indicate that steric repulsion and linker distortions are major components of lattice rigidity of MOFs.

The compression of porous materials is a complex phenomenon with many contributing factors. This systematic study demonstrates that—all other variables held constant—the void fraction and bulk modulus of MOFs are inversely related. Owing to rigorous experimental design, this trend is expected to apply to other examples outside of those discussed here, including other classes of MOFs and porous materials. However, this extensive investigation also reveals that slight structural differences (such as deviation from linear connectivity of the organic linker) greatly impact the bulk modulus of the material. These results highlight the need for further well-controlled, thorough studies into the role of other structural variables in order to construct a predictive model of pressure-induced structural changes and rigidity in these materials. This work is an important step toward developing a more complete, mechanistic understanding of compression in MOFs and, more broadly, porous materials.

## ASSOCIATED CONTENT

**Supporting Information.** Discussion of synthetic methods, ambient powder X-ray diffraction experiments, N<sub>2</sub> isotherm measurements, experimental details regarding *in situ* synchrotron powder X-ray diffraction experiments, details of Le Bail refinements, and discussion regarding distortions in UiO

MOFs at ambient pressure. “This material is available free of charge via the Internet at <http://pubs.acs.org>.”

## AUTHOR INFORMATION

### Corresponding Authors

\* Email: [o-farha@northwestern.edu](mailto:o-farha@northwestern.edu)

\* Email: [karena.chapman@stonybrook.edu](mailto:karena.chapman@stonybrook.edu)

### Notes

The authors declare no competing interests

## ACKNOWLEDGMENT

O.K.F. gratefully acknowledges support from the Defense Threat Reduction Agency (HDTRA1-18-1-0003). This research used resources of the Advanced Photon Source, a U.S. Department of Energy (DOE) Office of Science User Facility operated for the DOE Office of Science by Argonne National Laboratory under Contract No. DE-AC02-06CH11357. This material is based on work supported in part by the U.S. Department of Energy (DOE), Office of Science, Office of Workforce Development for Teachers and Scientists, Office of Science Graduate Student Research (SCGSR) program. The SCGSR program is administered by the Oak Ridge Institute for Science and Education (ORISE) for the DOE. ORISE is managed by ORAU under Contract DE-SC0014664. Use was made of the IMSERC X-ray Facility at Northwestern University, which has received support from the Soft and Hybrid Nanotechnology Experimental (SHyNE) Resource (NSF ECCS-1542205), the State of Illinois, and the International Institute for Nanotechnology (IIN).

## REFERENCES

1. Farha, O. K.; Özgür Yazaydın, A.; Eryazici, I.; Malliakas, C. D.; Hauser, B. G.; Kanatzidis, M. G.; Nguyen, S. T.; Snurr, R. Q.; Hupp, J. T., De Novo Synthesis of a Metal–Organic Framework Material Featuring Ultrahigh Surface Area and Gas Storage Capacities. *Nature Chemistry* **2010**, *2*, 944–948.
2. Ma, S.; Zhou, H.-C., Gas Storage in Porous Metal–Organic Frameworks for Clean Energy Applications. *Chem. Commun.* **2010**, *46*, 44–53.
3. Furukawa, H.; Cordova, K. E.; O’Keeffe, M.; Yaghi, O. M., The Chemistry and Applications of Metal–Organic Frameworks. *Science* **2013**, *341*, 1230–1244.
4. Li, J.-R.; Kuppler, R. J.; Zhou, H.-C., Selective Gas Adsorption and Separation in Metal–Organic Frameworks. *Chem. Soc. Rev.* **2009**, *38*, 1477–1504.
5. Lee, J.; Farha, O. K.; Roberts, J.; Scheidt, K. A.; Nguyen, S. T.; Hupp, J. T., Metal–Organic Framework Materials as Catalysts. *Chem. Soc. Rev.* **2009**, *38*, 1450–1459.
6. Moghadam, P. Z.; Li, A.; Wiggan, S. B.; Tao, A.; Maloney, A. G. P.; Wood, P. A.; Ward, S. C.; Fairen-Jimenez, D., Development of a Cambridge Structural Database Subset: A Collection of Metal–Organic Frameworks for Past, Present, and Future. *Chem. Mater.* **2017**, *29*, 2618–2625.
7. Schneemann, A.; Bon, V.; Schwedler, I.; Senkowska, I.; Kaskel, S.; Fischer, R. A., Flexible Metal–Organic Frameworks. *Chem. Soc. Rev.* **2014**, *43*, 6062–6096.
8. Zhang, Y.; Zhang, X.; Lyu, J.; Otake, K.-i.; Wang, X.; Redfern, L. R.; Malliakas, C. D.; Li, Z.; Islamoglu, T.; Wang, B.; Farha, O. K., A Flexible Metal–Organic Framework with 4-Connected Zr6 Nodes. *J. Am. Chem. Soc.* **2018**, *140*, 1179–1183.

9. Chapman, K. W.; Halder, G. J.; Chupas, P. J., Guest-Dependent High Pressure Phenomena in a Nanoporous Metal–Organic Framework Material. *J. Am. Chem. Soc.* **2008**, *130*, 10524–10526.
10. Moggach, S. A.; Bennett, T. D.; Cheetham, A. K., The Effect of Pressure on Zif-8: Increasing Pore Size with Pressure and the Formation of a High-Pressure Phase at 1.47 Gpa. *Angew. Chem. Int. Ed.* **2009**, *48*, 7087–7089.
11. Hazen, R. M.; Finger, L. W., Compressibility of Zeolite 4a Is Dependent on the Molecular Size of the Hydrostatic Pressure Medium. *J. Appl. Phys.* **1984**, *56*, 1838–1840.
12. Fois, E.; Gamba, A.; Medici, C.; Tabacchi, G.; Quartieri, S.; Mazzucato, E.; Arletti, R.; Vezzalini, G.; Dmitriev, V., High Pressure Deformation Mechanism of Li-Abw: Synchrotron Xrd Study and Ab Initio Molecular Dynamics Simulations. *Microporous Mesoporous Mater.* **2008**, *115*, 267–280.
13. Gatta, G. D.; Lee, Y., Zeolites at High Pressure: A Review. *Mineralogical Magazine* **2014**, *78*, 267–291.
14. Chapman, K. W.; Halder, G. J.; Chupas, P. J., Pressure-Induced Amorphization and Porosity Modification in a Metal–Organic Framework. *J. Am. Chem. Soc.* **2009**, *131*, 17546–17547.
15. Tan, J. C.; Bennett, T. D.; Cheetham, A. K., Chemical Structure, Network Topology, and Porosity Effects on the Mechanical Properties of Zeolitic Imidazolate Frameworks. *Proc. Natl. Acad. Sci. U. S. A.* **2010**, *107*, 9938.
16. Galvelis, R.; Slater, B.; Cheetham, A. K.; Mellot-Draznieks, C., Comparison of the Relative Stability of Zinc and Lithium-Boron Zeolitic Imidazolate Frameworks. *CrystEngComm* **2012**, *14*, 374–378.
17. Hughes, J. T.; Bennett, T. D.; Cheetham, A. K.; Navrotsky, A., Thermochemistry of Zeolitic Imidazolate Frameworks of Varying Porosity. *J. Am. Chem. Soc.* **2013**, *135*, 598–601.
18. Yot, P. G.; Yang, K.; Ragon, F.; Dmitriev, V.; Devic, T.; Horcajada, P.; Serre, C.; Maurin, G., Exploration of the Mechanical Behavior of Metal Organic Frameworks Uio-66(Zr) and Mil-125(Ti) and Their Nh<sub>2</sub> Functionalized Versions. *Dalton Transactions* **2016**, *45*, 4283–4288.
19. Bennett, T. D.; Cheetham, A. K.; Fuchs, A. H.; Coudert, F.-X., Interplay between Defects, Disorder and Flexibility in Metal–Organic Frameworks. *Nature Chemistry* **2016**, *9*, 11–16.
20. DeStefano, M. R.; Islamoglu, T.; Garibay, S. J.; Hupp, J. T.; Farha, O. K., Room-Temperature Synthesis of Uio-66 and Thermal Modulation of Densities of Defect Sites. *Chem. Mater.* **2017**, *29*, 1357–1361.
21. Bon, V.; Senkovska, I.; Weiss, M. S.; Kaskel, S., Tailoring of Network Dimensionality and Porosity Adjustment in Zr- and Hf-Based Mofs. *CrystEngComm* **2013**, *15*, 9572–9577.
22. Jiang, H.-L.; Feng, D.; Liu, T.-F.; Li, J.-R.; Zhou, H.-C., Pore Surface Engineering with Controlled Loadings of Functional Groups Via Click Chemistry in Highly Stable Metal–Organic Frameworks. *J. Am. Chem. Soc.* **2012**, *134*, 14690–14693.
23. Deria, P.; Gómez-Gualdrón, D. A.; Hod, I.; Snurr, R. Q.; Hupp, J. T.; Farha, O. K., Framework-Topology-Dependent Catalytic Activity of Zirconium-Based (Porphinato)Zinc(II) Mofs. *J. Am. Chem. Soc.* **2016**, *138*, 14449–14457.
24. Deria, P.; Yu, J.; Smith, T.; Balaraman, R. P., Ground-State Versus Excited-State Interchromophoric Interaction: Topology Dependent Excimer Contribution in Metal–Organic Framework Photophysics. *J. Am. Chem. Soc.* **2017**, *139*, 5973–5983.
25. Lammert, M.; Reinsch, H.; Murray, C. A.; Wharmby, M. T.; Terraschke, H.; Stock, N., Synthesis and Structure of Zr(IV)- and Ce(IV)-Based Cau-24 with 1,2,4,5-Tetrakis(4-Carboxyphenyl)Benzene. *Dalton Transactions* **2016**, *45*, 18822–18826.
26. Cambor, M. A.; Corma, A.; Valencia, S., Spontaneous Nucleation and Growth of Pure Silica Zeolite-B Free of Connectivity Defects. *Chem. Commun.* **1996**, *0*, 2365–2366.
27. Dissegna, S.; Vervoorts, P.; Hobday, C. L.; Düren, T.; Daisenberger, D.; Smith, A. J.; Fischer, R. A.; Kieslich, G., Tuning the Mechanical Response of Metal–Organic Frameworks by Defect Engineering. *J. Am. Chem. Soc.* **2018**, *140*, 11581–11584.
28. Islamoglu, T.; Ray, D.; Li, P.; Majewski, M. B.; Akpınar, I.; Zhang, X.; Cramer, C. J.; Gagliardi, L.; Farha, O. K., From Transition Metals to Lanthanides to Actinides: Metal-Mediated Tuning of Electronic Properties of Isostructural Metal–Organic Frameworks. *Inorg. Chem.* **2018**, *57*, 13246–13251.
29. Katz, M. J.; Brown, Z. J.; Colon, Y. J.; Siu, P. W.; Scheidt, K. A.; Snurr, R. Q.; Hupp, J. T.; Farha, O. K., A Facile Synthesis of Uio-66, Uio-67 and Their Derivatives. *Chem. Commun.* **2013**, *49*, 9449–9451.
30. Garibay, S. J.; Iordanov, I.; Islamoglu, T.; DeCoste, J. B.; Farha, O. K., Synthesis and Functionalization of Phase-Pure Nu-901 for Enhanced Co<sub>2</sub> Adsorption: The Influence of a Zirconium Salt and Modulator on the Topology and Phase Purity. *CrystEngComm* **2018**, *20*, 7066–7070.
31. Hobday Claire, L.; Marshall Ross, J.; Murphie Colin, F.; Sotelo, J.; Richards, T.; Allan David, R.; Düren, T.; Coudert, F.-X.; Forgan Ross, S.; Morrison Carole, A.; Moggach Stephen, A.; Bennett Thomas, D., A Computational and Experimental Approach Linking Disorder, High-Pressure Behavior, and Mechanical Properties in Uio Frameworks. *Angew. Chem. Int. Ed.* **2016**, *55*, 2401–2405.
32. Yang, K.; Zhou, G.; Xu, Q., The Elasticity of Mofs under Mechanical Pressure. *RSC Advances* **2016**, *6*, 37506–37514.
33. Howarth, A. J.; Liu, Y.; Li, P.; Li, Z.; Wang, T. C.; Hupp, J. T.; Farha, O. K., Chemical, Thermal and Mechanical Stabilities of Metal–Organic Frameworks. *Nat. Rev. Mater.* **2016**, *1*, 15018.
34. Hasegawa, M.; Young, W. H., Bulk Moduli of Solid and Liquid Metals. *Journal of Physics F: Metal Physics* **1981**, *11*, 977–994.
35. Lee, M. W., Elastic Velocities of Partially Gas-Saturated Unconsolidated Sediments. *Marine and Petroleum Geology* **2004**, *21*, 641–650.
36. Wu, H.; Yildirim, T.; Zhou, W., Exceptional Mechanical Stability of Highly Porous Zirconium Metal–Organic Framework Uio-66 and Its Important Implications. *The Journal of Physical Chemistry Letters* **2013**, *4*, 925–930.
37. Yang, Q.; Guillerm, V.; Ragon, F.; Wiersum, A. D.; Llewellyn, P. L.; Zhong, C.; Devic, T.; Serre, C.; Maurin, G., CH<sub>4</sub> Storage and CO<sub>2</sub> Capture in Highly Porous Zirconium Oxide Based Metal–Organic Frameworks. *Chem. Commun.* **2012**, *48*, 9831–9833.
38. Tagliabue, M.; Rizzo, C.; Millini, R.; Dietzel, P. D. C.; Blom, R.; Zanardi, S., Methane Storage on Cpo-27-Ni Pellets. *J. Porous Mater.* **2011**, *18*, 289–296.

